I-V Characteristics Observation of Graphene Boron Nitride Vertical Heterojunction Van der Waals Resonant Tunneling Diode

A Thesis Submitted

For the partial contentment for the Degree of

Bachelor of Science in Electrical and Electronic Engineering to the

Department of Electrical and Electronic Engineering

BRAC University

Dhaka-1212, Bangladesh

By

Saber Ahmed-(13121044)

Rifat Binte Sobhan-(13121126)

August 2016

Candidate Declaration

We hereby declare that the thesis titled "I-V Characteristics Observation of Graphene Boron Nitride Vertical Heterojunction Van der Waals Resonant Tunneling Diode" is submitted to the Department of Electrical and Electronic Engineering of BRAC University with the aim of completion for the degree of Bachelor of Science in Electrical and Electronic Engineering. The following work is our original productuion and has not submitted elsewhere for the award of any other degree, diploma or any kind of publication.

Date- 17^{th} August 2016

Atanu Kumar Saha

Thesis Supervisor

Authors:

Saber Ahmed

Student ID: 13121044

Rifat Binte Sobhan

Student ID: 13121126

Acknowledgment

Firstly, we would like to express our gratitude to our respected thesis supervisor, Atanu Kumar Saha, Lecturer, Department of Electrical and Electronic Engineering (EEE), BRAC University; for his supportive supervision and feedbacks during the completion and enabling us to develop the core concepts and guiding us throughout patiently. Next we would like to attribute our thankfulness towards BRAC University for providing us with resources required for the research, and every other individual without whose contribution, the research would not be a success.

Abstract

In this paper, we are going to observe the band structure and I-V characteristics of Graphene Boron Nitride Vertical Heterojunction Van der Waals Resonant Tunneling Diode. Furthermore, showing negative differential resistance (NDR) characteristics which is a very important features and advantage of resonant tunneling diodes (RTD).

I-V Characteristics Observation of Graphene Boron Nitride Vertical Heterojunction Van der Waals Resonant Tunneling Diode

Saber Ahmed, Rifat Binte Sobhan

Contents

List of Figures

1 Introduction

1.1 The Era of Tunneling Diode(TD)

For the fast operation in the electronic world tunneling diode (TD) was introduced by Leo Esaki at August 1957 [8]. TD provides same functionality as a CMOS transistor [1]. At a specific external bias voltage range the device conduct current by which the device switched on. The differences between CMOS and tunnel diode is in CMOS current going through source to drain and in tunnel diode current goes through the depletion region by tunneling [1]. A TD is a p and n type junction where high concentration of electrons in the conduction band of the n-type region and empty states in the valence band of p-type region. The forward voltage applied then Fermi level of n-type increase and Fermi level of p-type decrease thus electron flows. Depending on how many electrons in the n-type region are energetically aligned with the valance band of p- type the current will increase or decrease. At the reverse bias the electron of valance band of p-type region energetically aligned with the empty states of n-type region so large reverse bias tunneling current flows. I-V characteristics of tunneling diode given below.

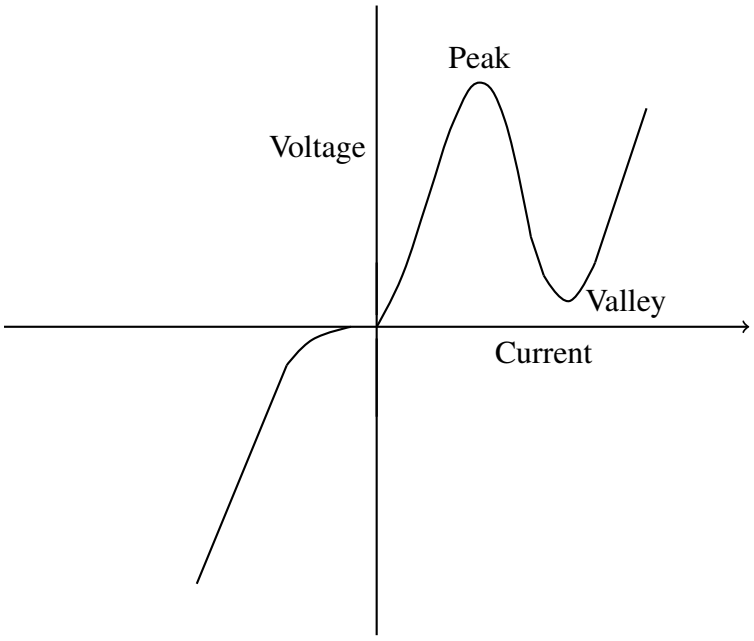

Figure 1: Characteristics of TD Diodes

1.2 Resonent Tunneling Diode(RTD)

Resonant tunneling diode (RTD) comes from the idea of TD. RTD gives faster operation than TD. Beside this there is a major advantage in RTD over TD and that is when a high reverse bias voltage is applied to TDs, there is very high leakage current and at the RTD side there we could find different amount of leakage current depending on the material used for the RTD.

1.3 Application Area of TD

As we have already known [1] that TD are considered more than useful in achieving ultrahigh speed in wide-band devices over the very accepted and current tran-

sistor technology CMOS. A special and practicable form of a TD is the RTD. It has resonant tunneling structure by which electrons are permitted to tunnel through in different resonant states at certain energy levels. Additionally it contains a very solitary property called Negative Differential Resistance (NDR) which is very large at room temperature [2].

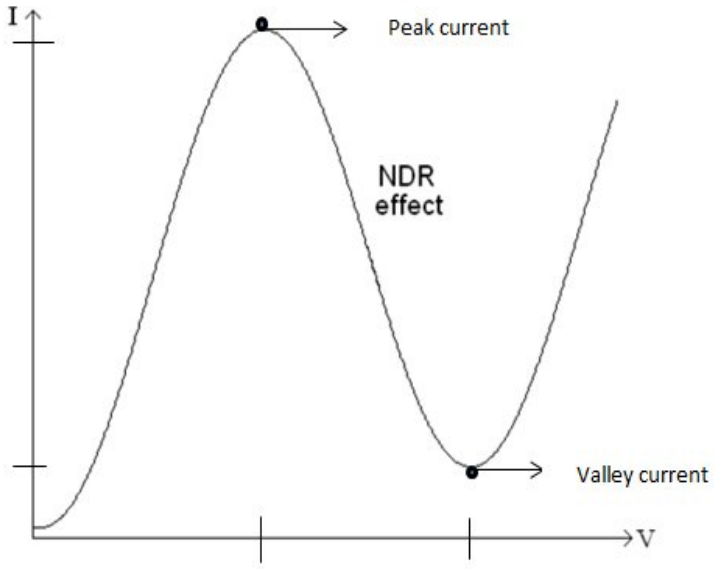

Figure 2: I-V characteristic of RTD showing NDR

1.4 Application Area of RTD

As we have informed that [3] RTD can be fabricated in different types of resonant tunneling structure such as heavily doped PN junction in Esaki diodes, double barriers and triple barriers along with various kinds of elements like as type IV, III-V, II-IV semiconductors.

1.5 Working Principle of RTD

In the device Figure3, a quantum well is enclosed by two tunnel barrier with large band gap material and a heavily doped emitter region with narrow energy gap materials and finally a collector region [1].

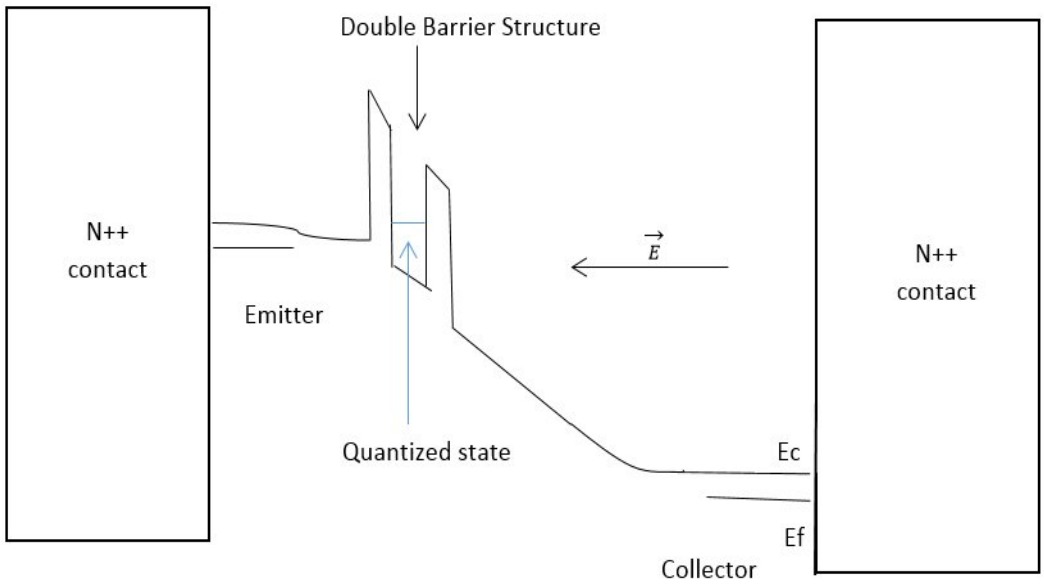

Figure 3: Structural diagram of RTD [1]

At low forward bias voltage, due to non-resonant, leakage current through surface states, scattering assisted tunneling along with thermionic emission small current flows. With the increment of biasing voltage as many electrons get close to the energy same as quasi energy state (Resonant level), those electrons start to tunnel through the scattering states within quantum-well from emitter to collector by creating an increased current, when the energy reached to Resonant level a highest current is achieved is called peak current and the phenomena is named Resonant tunneling. Resonant tunneling happens at specific resonant energy level

with particular doping level along with quantum wells width [1]. When the energy of the electrons of emitter side exceeds the quasi energy, current starts to decrease. And after a certain applied voltage, current starts to rise again. The minimum current is called Valley current or leakage current.

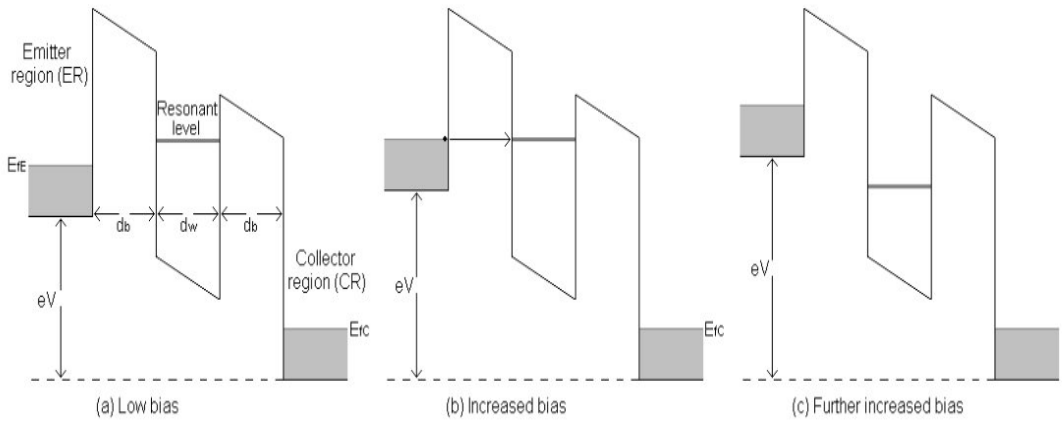

Figure 4: Band structure of RTD under different biasing [2]

1.6 Advantages of RTD over TD

As RTD has more advantages over TDs and CMOS technology so its application cover a wide area in the field of electronic. RTD got advantage when a reverse voltage is applied as it produces high leakage current and furthermore close to symmetrical I-V characteristics while both forward and reverse bias are applied. As we know [5] that RTD gives NDR, this NDR gives the opportunity to design bistability and positive feedback. Beside this because of this NDR facilities with RTD it is possible to create novel memories, multistage logic, oscillators and nu-

merous things that operates at low power and low voltage. Furthermore, [4] for ultrahigh speed analog and digital devices RTDs are considered as the most practical quantum effect device. From RTDs NDR facility ultrahigh speed Monostable-Bistable Transition Logic Element (MOBILE) can be deigned. Finally referred to [7], a recent discovery called Quantum MOS (Q-MOS) in the group of logic circuits has shown very low power delay profile and good noise immunity which is made by incorporating RTD with n-type transistors of conventional Complementary Metal Oxide Semiconductor (CMOS). CMOS circuit displays almost 20 percent slower sensing time compared to this RTD based Q-MOS sensing circuit.

2 Material Study

Graphene, a two-dimensional single-atom thick membrane of carbon atoms arranged in a honeycomb crystal, has been the most widespread material due to its excellent electrical, magnetic, thermal, optical and mechanical properties. Bilayer graphene is also an important material as it has very unique electronic structure as well as transport properties. On the other hand, Boron Nitride, a hexagonal lattice consisting of analogous structure as graphene has recently attracted much attention due to its superior mechanical and thermal conducting properties. Though both were discovered in the same century the difficulties of different production techniques and high cost of BN has limited its fabrication practices for about hundred years. In contrast to the zero bandgap of graphene, BN Nano Ribbons exhibit a wide bandgap suitable for semiconductors, optoelectronics and dielectric substrate for high-performance graphene electronics. Graphene sandwiched by monolayer BN is predicted to have a tunable bandgap without sacrificing its mobility.

2.1 Lattice Structure and orbital hybridization of Graphene and BN

Both Graphene and Boron Nitride are defined by sp^2 hybridization. sp^2 hybridized orbital is responsible for bonding in p_x and p_y orbital of graphene and remaining p_z orbital is situated perpendicularly to that plane. This perpendicular orbital contributes one conducting electron for per carbon atom. Thus among these four valence orbitals (2s,$2p_x$,$2p_y$,$2p_z$) of carbon atom the s ,p_x,p_y orbitals

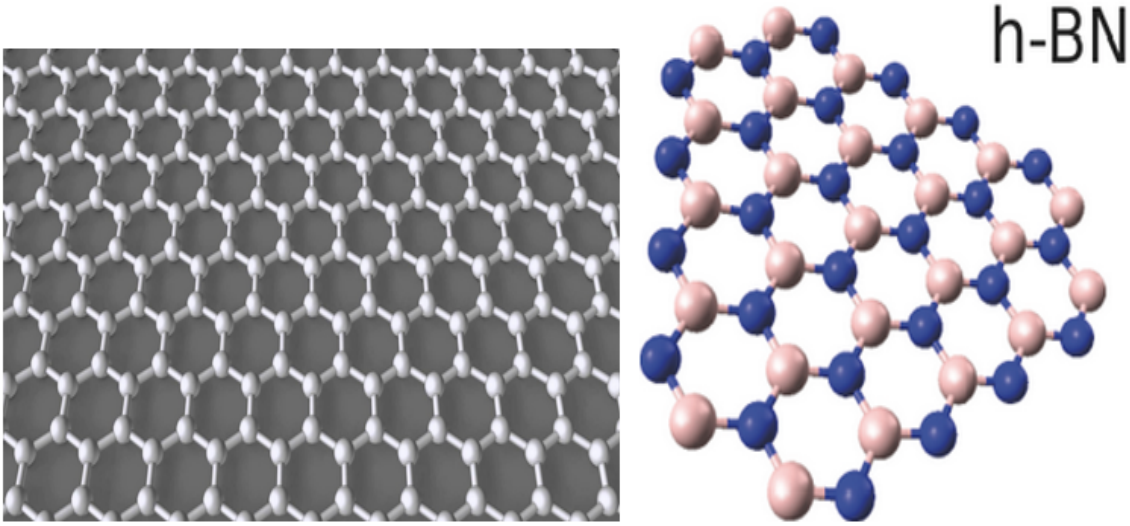

Figure 5: Atomic Structure of Graphene and Boron Nitride[9]

combine to form the in-plane occupied orbital (σ) and unoccupied orbital(σ^*). These orbitals are even planner symmetry. The p_z orbital which is an odd planner symmetry forms localized π and π^* orbital. The bonding orbitals are strongly covalent bonds determining the energetic stability and the elastic properties of Graphene. The remaining p_z orbital is odd with respect to the planner symmetry and decoupled from the bonding states. From the lateral interaction with neighboring p_z orbitals, localized π and π^* orbitals are formed. Graphite consists of a stack of many Graphene layers. The unit cell in Graphene can be primarily defined using two graphene layers translated from each other by a C-C distance, $a_(c-c)$=1.42. The three-dimensional structure of Graphite is maintained by weak interlayer Van Der Waals interaction between bond so adjacent layers, which generate a weak but finite out-of-plane delocalization. Boron having electronic

structure of $1s^2\ 2s^2\ 2p^1$ along with nitrogen with an electronic structure of $1s^2\ 2s^2$

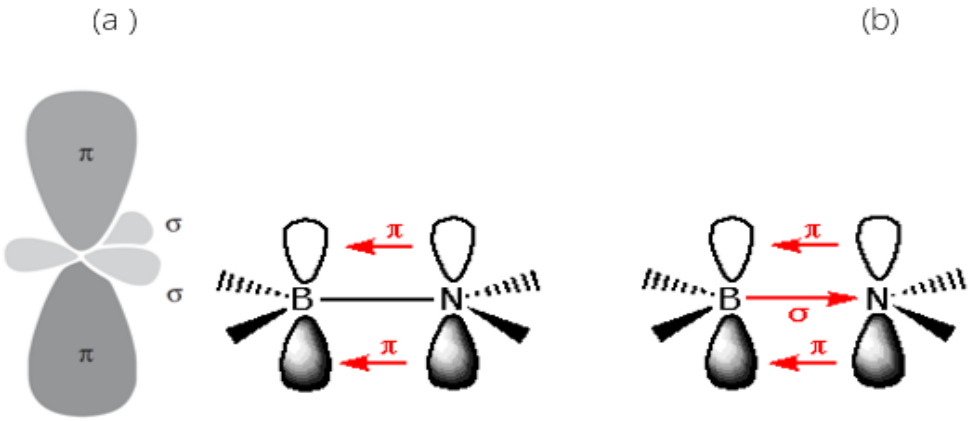

Figure 6: (a) sp2 Hybridization of Graphene, (b) sp2 Hybridization of BN[10]

$2p^3$, forms sp^2 hybrid bonds in the B-N sheets. In sp^2h ybridization Boron uses all of the outer electrons to give the configuration $1s^1$ $2p_x^1$ $2p_y^1$ $2p_z^2$when fabricated with Nitrogen. After formation of the sp^2orbital, the remaining two p electrons are located in the (filled) p_z orbital. The σ bonding in the BN sheets that result is strong and similar to the bonding in the graphite sheets. However, π bonding between the full $2p_z$ orbitals of nitrogen and the empty $2p_z$ orbitals of boron is not possible. This is because the orbital energies of boron and nitrogen are too dissimilar for a large energy gain. Thus no delocalized electron is present in the structure. Because of this the boron and nitrogen atoms in alternate layers avoid each other. This allows for the more efficient packing of the filled p_z orbitals, and the layers are closer than they are in graphite. Nevertheless, the lack of bonding between the layers still means that BN retains the easy cleavage of graphite and still is a good dry lubricant.

2.2 Energy Dispersion Relation of Graphene and Boron Nitride

Graphene, a single atomic sheet of periodically arranged graphite forming an infinite honeycomb lattice, is a two-dimensional allotrope having a single layer of sp^2 -bonded carbon atoms that are densely packed. Ever since the first demonstration of its zero bandgap, the lattice has attracted much attention not only for its exceptional strength and thermal conductivity but also for electrical conductivity. Since Carbon (C), Boron (B) and Nitrogen (N) are all in the same period of the periodic table, single layer hexagonal Boron Nitride (h-BN) exhibits analogous honeycomb structure as Graphene and also has distinct bandgap variation trends. Moreover, the band structure and energy dispersion relation of Graphene and BN provides better understanding in analyzing the possibilities of opening a tunable bandgap when Graphene Nano Ribbons (GNR) are embedded in BN Nano Ribbons (BNNR). Among all possible band structure calculation methodologies Density Functional Theory (DFT) and nearest Tight Binding (TB) method have been employed in this paper in order to find appropriate bandgap.[11-14]

2.2.1 Introduction to DFT (Density Functional Theory)

Since 1970s Density functional theory (DFT) has been considered the most versatile method for quantum mechanical calculation. However it did not get complete recognition until the year of 1990s. In the following year the approximations used in theory was redefined to such an extent that they satisfactorily agreed with the experimental data, especially the ones attained from first principles calculation. Hence, DFT has been defined as the quantum mechanical modelling method used

to investigate the electronic band structure as well as other electronic properties of atoms, molecules and condensed phases. Using this theory, the properties of a many-electron system can be evaluated specially the ones dependent on electron density. The name Density Functional Theory has been driven from the fact that DFT incorporates the use of functionals of the electron density. Compared to costly methods like first principles calculation or Hartree-Fock theory DFT is much cost-effective. [15]

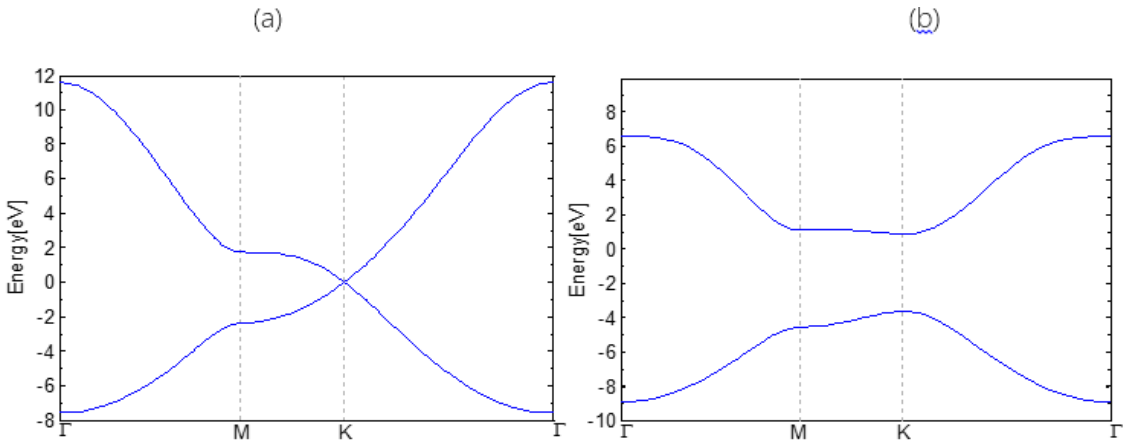

Figure 7: (a) Band Structure of Graphene using DFT calculation. (b) Band Structure of BN using DFT calculation.

2.2.2 Introduction to nearest neighbor TB (Tight Binding) model

Tight-binding models are applied to a wide variety of matters and they give good qualitative results in many cases. The nearest TB model is defined as an approach that calculates electronic band structures using an approximate set of wave functions based on superposition of wave functions for isolated atoms located at each atomic site. It is closely related to the Linear Combination of Atomic Orbitals method (LCAO).TB overlap as well as Hamiltonian matrices directly from first-principles calculations has always been a subject of continuous interest. Since, the nearest TB model primarily attempts to represent the electronic structure of condensed matter using a minimal atomic-orbital like basis set; it has been redefined to fit the resultants of first-principles calculations.

Usually, first-principles calculations are done using a large or long-ranged basis set in order to get convergent results, while tight-binding overlap and Hamiltonian matrices are based on a short-ranged minimal basis representation. Therefore in this paper, we performed a transformation that can carry the electronic Hamiltonian matrix from a large or long-ranged basis representation onto a short ranged minimal basis representation in order to obtain an accurate tight-binding Hamiltonian from first principles calculation.[16]

2.2.3 Band Structure (E-k relation) calculation

Electronic band structure of a matter is described by the ranges of energy that an electron within the matter may have and also the ranges of energy that it may not have (called band gaps or forbidden bands). By examining the allowed quantum mechanical wave functions for an electron in a large, periodic lattice of atoms or molecules, the electronic bands and band gaps can effectively be derived. Again

by knowing the band structures of Graphene and 2D h-BN lattice, their future possibilities in making better Nano-scaled devices can easily be comprehended. Since ab-initio DFT method effectively represents first principles calculation, the parameters of nearest TB model have been modified to follow the variation trends of DFT calculation. Therefore, for electronic band gap calculation DFT and Nearest TB model have been employed in this paper.

From First principles calculations it has been observed that the electronic bands near the Fermi level are contributed from the orbitals of the atoms. Thus a π -orbital nearest TB model has been engaged to investigate quantum confinement as well as edge effects on the electronic band structure of both Graphene and BN. Compared to the time consuming First principles calculation, this modified nearest TB method can be effectively applied to study more intricate low dimensional Nano structures whose properties are controlled by π electrons.

To attain the π-orbital nearest TB Hamiltonian and derive the electronic spectrum of the total Hamiltonian, the corresponding Schrodinger equation has to be solved. According to time-independent Schrodinger's equation:[16,17-19]

$$E(\vec{K})\psi(\vec{K},\vec{r}) = \hat{H}\psi(\vec{K},\vec{r}) \tag{1}$$

where,

$\hat{H}$=$H_o p$=Hamiltonian operator

E= Eigen Energy (expectation value of the orbital energy

ψ=Eigen function (molecular orbital wave function

Because of translational symmetry in a particular lattice the molecular Eigen functions can be written as the linear combination of atomic Eigen functions ψ(j=1,2,3,.....,n); where n is the number of Bloch wave functions) and Bloch or-

bital (appendix) basis functions $a_j(\vec{r})$:

$$\psi_M = \sum_{j=1}^{n} \psi_j a_j \tag{2}$$

However, this Linear Combination of Atomic Orbital (LCAO) gives approximate solution instead of exact solution of the Schrodinger's equation. Thus we incorporated the Variational principal where, for a particular wave function, the expected value of orbital energy or Eigen energy is given by:

$$E = \frac{\int \psi^* \hat{H} \psi dr}{\int \psi^* \psi dr} \tag{3}$$

The following principle also states that the value of E obtained by using equation (1) is always greater than that of the exact solution.

General form of equation:

$$E\psi_n = \sum_m H_{nm}\psi_m \tag{4}$$

For both 2D and 3D lattice: $\psi_n = \psi_0 e^{\vec{k}.\vec{r}_n}$; where $\vec{r}_n$ is the position (position vector) of the n^{th} atom. To calculate $E(k)$ relation for 2D or 3D lattice the following equation is formed:

$$E\psi_0 e^{i\vec{k}\vec{r}_n} = \sum_m H_{mn}\psi_0 e^{i\vec{k}\vec{r}_m} \tag{5}$$

$$E\psi_0 = \sum_m H_{mn}\psi_0 e^{i\vec{k}(r_m \vec{-} r_n)} \tag{6}$$

$$E = \sum_m H_{mn} e^{i\vec{k}(r_m \vec{-} r_n)} \tag{7}$$

$$E(\vec{k}) = \sum_m H_{mn} e^{i\vec{k}(r_m \vec{-} r_n)} \tag{8}$$

Here, (r_m-r_n) is the vector that runs from m^{th} atom to n^{th} atom.

Self-integrals can be defined as, $\epsilon = \left\langle \epsilon_n \middle| \hat{H} \middle| \epsilon_n \right\rangle$

Hopping integrals can be defined as,$t = \left\langle \epsilon_(n-1) \middle| \hat{H} \middle| \epsilon_n \right\rangle$ or $\left\langle \epsilon_n \middle| H \middle| \epsilon_(n+1) \right\rangle$

2.2.4 Energy Dispersion (E-k relation) calculation of Graphene

Carbon atoms in a Graphene plane are located at the vertices of a hexagonal lattice where each C atom is surrounded by three C atoms.

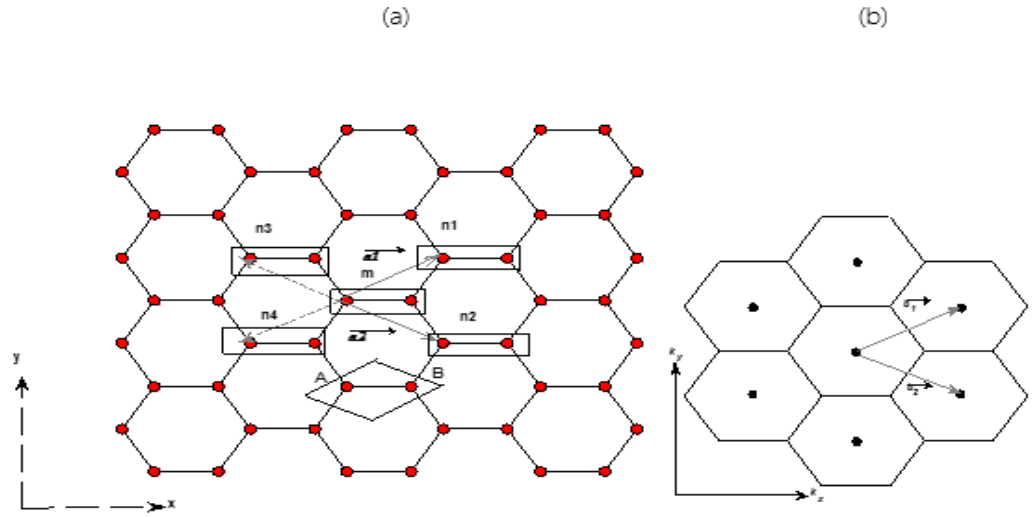

Figure 8: (a) Real Space Lattice of Graphene, (b) Reciprocal Space Lattice of Graphene.

From the figure-8, Graphene network can be regarded as a triangular Bravais lattice with two atoms (A and B) per unit cell along with basis vectors a_1 and a_2, where

$\hat{a}_1 = \frac{\sqrt{3}}{2}\hat{a}_x + \frac{1}{2}\hat{a}_y$;(First Primitive Vector)

$\hat{a}_2 = \frac{\sqrt{3}}{2}\hat{a}_x - \frac{1}{2}\hat{a}_y$;(Second Primitive Vector)

Here,$a = \sqrt{3}a_{(C-C)}$,where $a_{(C-C)}$=1.42 is the carbon-carbon distance in graphene.

At figure we can see that each A or B-type atom is surrounded by three opposite type. By using condition $a_i.b_j = 2\pi\delta_{ij}$, the reciprocal lattice vectors ($\hat{b}_1$ and

$\hat{b}_2$) can be obtained where,

$\hat{b}_1 = b(\frac{1}{2}\hat{k}_x + \frac{\sqrt{3}}{2}\hat{k}_y)$

$\hat{b}_2 = b(\frac{1}{2}\hat{k}_x - \frac{\sqrt{3}}{2}\hat{k}_y)$

where $b = \frac{4}{a\sqrt{3}}$. In figure-9 these vectors will be shown. The hexagonal shaped Brillouin zone is built as the Wigner-Seitz cell of reciprocal lattice. Out of its six corners, two of them are equivalent (the others can be written as one of these two plus a reciprocal lattice vector).

If carbon atoms are placed onto the Graphene hexagonal network the electronic wavefunctions from different atoms overlap. Because of symmetry the overlap between the p_z orbitals and the s or the p_x and p_y electrons are strictly zero.

The p_z electrons form the π bonds in Graphene can be treated independently from other valence electrons. Within this π-band approximation, the A-atom or B-atom is uniquely defined by one orbital per atom site p_z $(\hat{r} - \hat{r}_A)$ or $p_z(\hat{r} - \hat{r}_B)$.

From Blochs theorem, the Eigen-functions evaluated at two given Bravais lattice points $\hat{r}_m$and $\hat{r}_n$ differ from each other in just a phase factor, $e^{(ik(\hat{r}_m - \hat{r}_n))}$.By using the orthogonality relation in the Schrodinger equation, $H\psi = E\psi$, the energy dispersion relation we can be easily obtained from the diagonalization of $E(\hat{K})$. For calculating the dispersion relation of Graphene lattice two C-C molecules m and n1 are considered first. $E(k_x, k_y)$ or E is considered to be the energy of the system depending on the k vector.

Since from secular eguation it has been obtained that ϵ are the site energies of carbon, thus C-C self-iteration (for A type-A or B type-B type)=ϵ

And (A type -B type) hopping integral=t

In matrix form the diagonal elements become :

$$\begin{bmatrix} \epsilon & t \\ t & \epsilon \end{bmatrix}$$

similarly, the iterations$(m-n_1)$,$(m-n_2)$ form upper diagonal matrix

$$\begin{bmatrix} 0 & 0 \\ t & 0 \end{bmatrix}$$

and (m-n3),(m-n4) form lower diagonal matrix

$$\begin{bmatrix} 0 & t \\ 0 & 0 \end{bmatrix}$$

Therefore taking $\hat{a}_1$ and $\hat{a}_2$ into account relation given by:

$$E(K) = \begin{bmatrix} 0 & t \\ 0 & 0 \end{bmatrix} e^{-i\vec{k}\hat{a}_2} + \begin{bmatrix} 0 & t \\ 0 & 0 \end{bmatrix} e^{-i\vec{k}\hat{a}_1} + \begin{bmatrix} \epsilon & t \\ t & \epsilon \end{bmatrix} + \begin{bmatrix} 0 & 0 \\ t & 0 \end{bmatrix} e^{-i\vec{k}\hat{a}_1} + \begin{bmatrix} 0 & 0 \\ t & 0 \end{bmatrix} e^{-i\vec{k}\hat{a}_2}$$

$$\begin{bmatrix} \epsilon & t + te^{-i\vec{k}\hat{a}_1} + te^{-i\vec{k}\hat{a}_2} \\ t + te^{i\vec{k}\hat{a}_1} + te^{i\vec{k}\hat{a}_2} & \epsilon \end{bmatrix}$$

Here,

$$E(\vec{k}) = \epsilon \pm |h_0| \text{ where } h_0 = t + te^{i\vec{k}\hat{a}_1} + te^{i\vec{k}\hat{a}_2}$$

$$h_0 = t(1 + e^{i\vec{k}\hat{a}_1} + e^{i\vec{k}\hat{a}_2})$$

$$h_0 = t(1 + e^{i\vec{k}(\hat{a}_x + \hat{b}_y)} + e^{i\vec{k}(\hat{a}_x - \hat{b}_y)})$$

$$h_0 = t(1 + e^{i\vec{k}_x a_x + i\vec{k}_y b_y} + e^{i\vec{k}_x a_x - i\vec{k}_y b_y})$$

$$h_0 = t(1 + e^{i\vec{k}_x a}(e^{i\vec{k}_y b_y} + e^{-i\vec{k}_y b_y}))$$

$$h_0 = t(1 + e^{i\vec{k}_x a} 2\cos\vec{k}_y b)$$

$$h_0 = t(1 + 2\cos\vec{k}_y b\cos\vec{k}_x a + 2i\cos\vec{k}_y b\sin\vec{k}_x a)$$

$$|h_0| = \sqrt{(1 + 2\cos\vec{k}_y b\cos\vec{k}_x a)^2 + (2\cos\vec{k}_y b\sin\vec{k}_x a)^2}$$

$$|h_0| = \sqrt{1 + 4\cos\vec{k}_y b\cos\vec{k}_x a + 4\cos^2\vec{k}_y b(\sin^2\vec{k}_x a + \cos^2\vec{k}_x a)}$$

Now,

$$a = \frac{3}{2}a_0 \text{ and } b = \frac{\sqrt{3}}{2}a_0$$

$$E(\vec{k}) = \epsilon \pm \sqrt{1 + 4\cos\vec{k}_y\frac{\sqrt{3}}{2}a_0\cos\vec{k}_x\frac{3}{2}a_0 + 4\cos^2\vec{k}_y\frac{\sqrt{3}}{2}a_0}$$

Using the equation the hexagonal shaped Brillouin zone of graphene can be obtained, the k_+,K_- and M valley are shown in figure-10. the center is denoted as Gamma(Γ) valley.

The wave-vector $k = (k_x, k_y)$ are chosen within the first hexagonal Brillouin zone . the zeros of $h_0(k)$ correspond to the crossing of the bands with the + and - signs. one can verify that $h_0(k = k_+) = h_0(k = k_-) = 0$ and therefore the crossing over occurs at the points k_+ and k_-. furthermore, with a single p_z electron per atom in the $-*$ model (the three other s, p_x,p_y fill the low-lying band), the (-) band (negative energy band) is fully occupied, while the (+) band (positive energy band) is empty, at least for electrically neutral Graphene. Thus, the fermi level E_F (charge neutrality point) in the zero-energy reference in fig-9

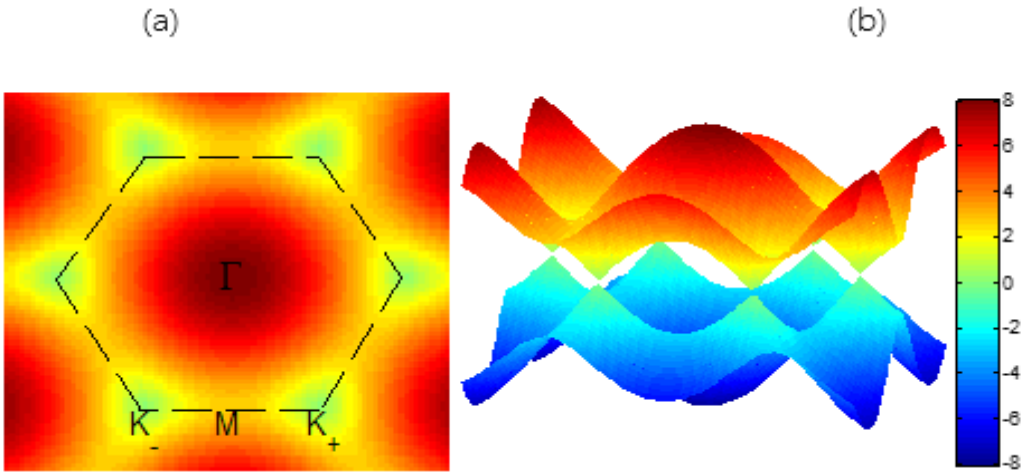

Figure 9: (a) First Brillouin zone (BZ) of graphene. (b) Energy dispersion relation of graphene.

and fermi surface is composed of the set of k_+ and k_- points. Thereby, Graphene displays a metallic (zero-bandgap) character. However, as the Fermi surface is of zero dimensions (since it is reduced to a discrete and finite set of points), the term semi-metal or zero-gap semiconductor is usually employed. Expanding for kin the vicinity of k_+ or k_-, $k = k + k$ or $k = k - k$, yields a linear dispersion for the and $*$ bands near these six corners of 2D hexagonal Brillouin Zone.

2.2.5 Band Structure and Energy Dispersion Calculation of BN

B and N atoms in a BN plane are located at the vertex of a hexagonal lattice where each B is surrounded by three N atoms and each N is surrounded by three B atoms. The following BN network in Figure-10 can be regarded as a triangular Bravais lattice with two atoms (one B and one N) per unit cell along with basis

vectors $\hat{a}_1$ and $\hat{a}_2$ where

$$\hat{a}_1 = \frac{\sqrt{3}}{2}\hat{a}_x + \frac{1}{2}\hat{a}_y \text{ (First primitive vector)}$$
$$\hat{a}_2 = \frac{\sqrt{3}}{2}\hat{a}_x - \frac{1}{2}\hat{a}_y \text{ (First primitive vector)}$$

Here, $a = \sqrt{3}a_{B-N}$, where $a_{B-N} = 2.512\mathring{A}$ is the Boron-Nitrogen distance in BN. $2D\ h-BN$ exhibits similar Brillouin zone formation due to its analogous structure as Graphene. According to Blochs theorem, the Eigen-functions evaluated at two given Bravais lattice points $\vec{r}_m$ $\vec{r}_n$ and differ from each other in just a phase factor,$e^{i\vec{k}(\vec{r}_m-\vec{r}_n)}$.Using the orthogonality relation in the Schrodinger equation, $H\Psi = E\Psi$, the energy dispersion relation can be easily obtained from the diagonalization of Energy dispersion relation.

For calculating the E(k) dispersion relation of $2D\ h-BN$ lattice two BN molecules m and n_1 (as shown in the Figure-11) are considered first. $E(k_x, k_y)$ or E is considered to be the energy of the system depending on the k vector. Since from secular equation it has been obtained that ϵ_B and ϵ_N are the Site energies of Boron and Nitrogen respectively,

$B-B$ self-interaction= $\epsilon_B - E(k_x, k_y) = \epsilon_B - E$

$N-N$ self-interaction = $\epsilon_N - E(k_x, k_y) = \epsilon_N - E$

And $B-N$ hopping integral= t

In matrix form the diagonal elements become:

$$\begin{bmatrix} \epsilon_B - E & t \\ t & \epsilon_N - E \end{bmatrix}$$

As the interaction $(m-n_1)$,$(m-n_2)$ form upper diagonal matrix

$$\begin{bmatrix} 0 & 0 \\ t & 0 \end{bmatrix}$$

and $(m-n_3)$,$(m-n_4)$ form lower diagonal matrix

$$\begin{bmatrix} 0 & t \\ 0 & 0 \end{bmatrix}$$

Now, by considering $\hat{a}_1$ and $\hat{a}_2$ the equation will be,

$$E(K) = \begin{bmatrix} 0 & t \\ 0 & 0 \end{bmatrix} e^{-i\vec{k}\hat{a}_1} + \begin{bmatrix} 0 & t \\ 0 & 0 \end{bmatrix} e^{-i\vec{k}\hat{a}_2} + \begin{bmatrix} \epsilon_B - E & t \\ t & \epsilon_N - E \end{bmatrix} + \begin{bmatrix} 0 & 0 \\ t & 0 \end{bmatrix} e^{i\vec{k}\hat{a}_1} + \begin{bmatrix} 0 & 0 \\ t & 0 \end{bmatrix} e^{i\vec{k}\hat{a}_2}$$

$$\begin{bmatrix} \epsilon_B - E & t + te^{-i\vec{k}\hat{a}_1} + te^{-i\vec{k}\hat{a}_2} \\ t + te^{i\vec{k}\hat{a}_1} + te^{i\vec{k}\hat{a}_2} & \epsilon_N - E \end{bmatrix}$$

$|E(K)| = 0$ (determinant of $E(K)$ is zero) gives the equation the following form :

$$(\epsilon_B - E).(\epsilon_N - E) - t^2(1 + e^{-ik\hat{a}_1} + e^{-ik\hat{a}_2})(1 + e^{ik\hat{a}_1} + e^{ik\hat{a}_2}) = 0)$$

$$(\epsilon_B)(\epsilon_N) - E\epsilon_B - E\epsilon_N + E^2 - t^2(1 + e^{-ik\hat{a}_1} + e^{-ik\hat{a}_2})(1 + e^{ik\hat{a}_1} + e^{ik\hat{a}_2}) = 0$$

Considering the part of the upper equation

$$(1 + e^{-ik\hat{a}_1} + e^{-ik\hat{a}_2})(1 + e^{ik\hat{a}_1} + e^{ik\hat{a}_2})$$

$$1 + e^{-ik\hat{a}_1} + e^{-ik\hat{a}_2} + e^{-ik\hat{a}_1} + (e^{ik\hat{a}_1}e^{-ik\hat{a}_1})...(e^{-ik\hat{a}_2}e^{ik\hat{a}_1}) + e^{ik\hat{a}_2} + (e^{-ik\hat{a}_1}e^{ik\hat{a}_2}) + (e^{-ik\hat{a}_2}e^{-ik\hat{a}_2})$$

$$1 + (e^{ik\hat{a}_1} + e^{-ik\hat{a}_1})...(e^{ik\hat{a}_2} + e^{-ik\hat{a}_2}) + 1 + (e^{-ik\hat{a}_2}e^{ik\hat{a}_1}) + 1 + e^{ik\hat{a}_1}e^{-ik\hat{a}_1}$$

$$3 + 2\cos k\hat{a}_1 + 2\cos k\hat{a}_2 + (e^{ik(\hat{a}_1 - \hat{a}_2))} + (e^{-ik(\hat{a}_1 - \hat{a}_2)})$$

$$3 + 2(\cos k\hat{a}_1 + \cos k\hat{a}_2 + 2\cos k(\hat{a}_1 - \hat{a}_2))$$

$$3 + 2(2\cos k\frac{(\hat{a}_1 + \hat{a}_2)}{2}\cos k\frac{(\hat{a}_1 - \hat{a}_2)}{2}) + 2\cos k(\hat{a}_1 - \hat{a}_2)$$

substituting the values of the primitive vectors,$\hat{a}_1 + \hat{a}_2 = \sqrt{3}\hat{a}_x$ and $\hat{a}_1 - \hat{a}_2 = \hat{a}_y$ leads the equation to as follows:

$$(1 + e^{-ik\hat{a}_1} + e^{-ik\hat{a}_2})(1 + e^{ik\hat{a}_1}...e^{ik\hat{a}_2}) =$$
$$3 - 4\cos k\frac{\sqrt{3}}{2}\hat{a}_x\cos k\frac{1}{2}\hat{a}_y + 2(2\cos k0.5\hat{a}_y - 1)$$

$$1 + 4\cos k\frac{\sqrt{3}}{2}\hat{a}_x\cos k0.5\hat{a}_y + 4(\cos k0.5\hat{a}_y)^2$$

So the equation will become,

$$\epsilon_B\epsilon_N - E\epsilon_B - E\epsilon_N + E^2 - t^2(1 + 4\cos k\frac{\sqrt{3}}{2}\hat{a}_x\cos k\frac{1}{2}\hat{a}_2 + 4\cos k\frac{1}{2}\hat{a}_y) = 0$$

$$E^2(\epsilon_B + \epsilon_N) + \epsilon_B\epsilon_N - t^2(1 + 4\cos k\frac{\sqrt{3}}{2}\hat{a}_x\cos k\frac{1}{2}\hat{a}_2 + 4\cos k\frac{1}{2}\hat{a}_y) = 0$$

$$E(k_x, k_y) =$$
$$\frac{(\epsilon_B + \epsilon_N) \pm \sqrt{(-(\epsilon_B + \epsilon_N))^2 - 4(\epsilon_B\epsilon_N - t^2(1 - 4\cos k\frac{\sqrt{3}}{2}\hat{a}_x\cos k\frac{1}{2}\hat{a}_y + 4\cos^2 k\frac{1}{2}\hat{a}_y))}}{2}$$

$$\frac{(\epsilon_B + \epsilon_N)}{2} \pm$$
$$\frac{1}{2}\sqrt{\epsilon_B^2 + \epsilon_N^2 + 2\epsilon_B\epsilon_N + 16t^2(\frac{1}{4} + \cos k\frac{\sqrt{3}}{2}\hat{a}_x\cos k\frac{1}{2}\hat{a}_y + \cos^2 k\frac{1}{2}\hat{a}_y)}$$

$$\frac{(\epsilon_B + \epsilon_N)}{2} \pm \frac{1}{2}\sqrt{(\epsilon_B - \epsilon_N)^2 + 16t^2(\frac{1}{4} + \cos k\frac{\sqrt{3}}{2}\hat{a}_x\cos k\frac{1}{2}\hat{a}_y + \cos^2 k\frac{1}{2}\hat{a}_y)}$$

So the equation become

$$E(k_x, k_y) =$$
$$\frac{(\epsilon_B + \epsilon_N)}{2} \pm \sqrt{\frac{(\epsilon_B - \epsilon_N)^2}{4} + 4t^2(\frac{1}{4} + \cos k\frac{\sqrt{3}}{2}\hat{a}_x \cos k\frac{1}{2}\hat{a}_y + \cos^2 k\frac{1}{2}\hat{a}_y)}$$

Using this equation hexagonal shaped Brillouin zone of BN can be obtained, where out of six corners two of them are equivalent. These two special points are denoted with K_+ and K_-. The center is denoted as Gamma (Γ) valley at figure-10.

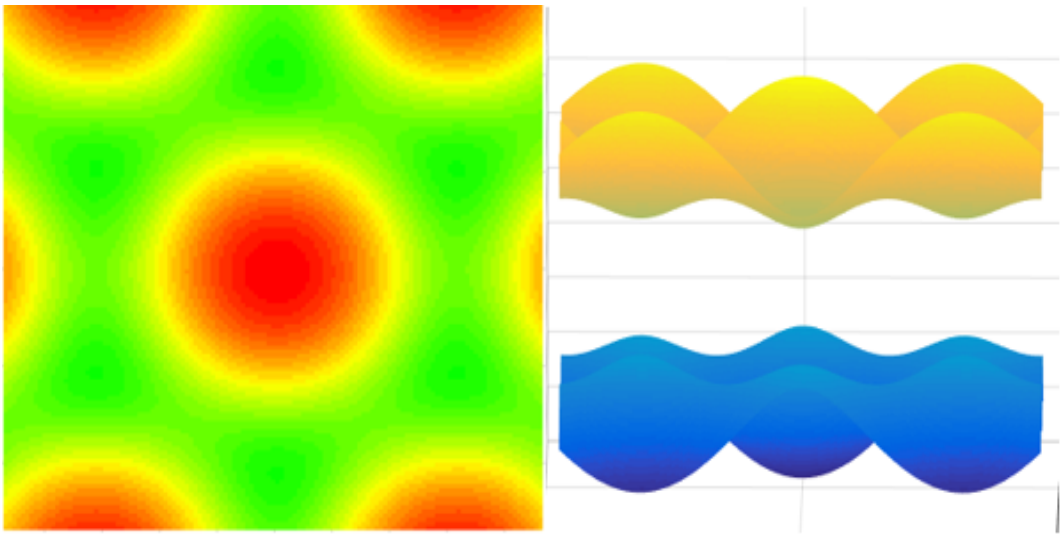

Figure 10: From Left, Brillouin Zone of hBN and Energy Dispertion Relation of hBN

3 Proposed Model of RTD Device

In our work we use the self-consistent capacitive model to create the RTD by using graphene and hBN layers. At the both top and bottom gate we use SiO2 oxide and our model consists of two tunneling channel made of layered hBN sandwiched between three graphene layers as shown in the figure as following the work of Jing Guo [6]. Here graphene layers works as source and drain contacts. From the work of Jing Guo [6] we see that there only two graphene layers used with sandwiched one layer of hBN to create the tunneling graphene heterojunction which will work as like TDs. Here we use three graphene layers with two hBN sandwiched layers whereas the two hBN layers will act as two tunneling channel as a result this device will work like RTDs. When bias voltage given then depending on the electron concentration of graphene layers the electrons will resonantly tunnel through the layers. At the previous works model [6] we see that at the forward bias voltage condition high current flows through the device, on the other hand on our modeled device we get both voltage peak and valley and thus our model show negative differential resistance (NDR) characteristics which is a very important features and advantage of resonant tunneling diodes (RTD). On the reverse bias voltage condition from the Jing Guos [6] work we see that high leakage current flows but as we make the device work like RTD so in our model we found a controlled leakage current.

3.1 Principle of Our Device

To explore the qualitative characteristics of theoretically modeled Vertical Tunneling Graphene field effect transistor (VTG-FET) and for further device escalation,

a self-consistent capacitance model is used. In addition to that the electrochemical potential profile across the gadget is achievable from the mentioned model. Soon after that, non-equilibrium-greens-function is used to enumerate current and conductance across the device. The modulation of density of states in the contacts fundamentally regulates the operations of the device whereas conventional transistor depends on source-drain contacts. An important note is DOS of contacts rely on applied gate voltage and source-drain voltage [6].

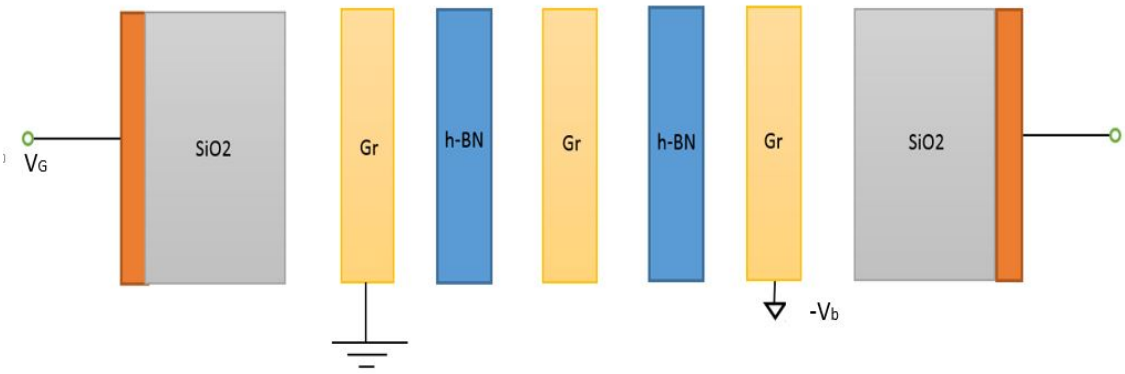

Figure 11: Layer Diagram of the RTD device

3.2 Capacitance Model

To estimate the electrochemical potential at graphene and hBN, a self-consistent capacitance model is used. In a few minutes, we are going to show the calculation for the device with the channel consisting of hBNs. The charge Qi at each layer-i

is related to vacuum energy level, Ei as showing in below.

$$-Q_i = C_i(E_{i-1}^{vac} - E_i^{vac}) + C_{i+1}(E_{i+1}^{vac} - E_i^{vac}); i = 0, 1, 2, 3, 4, ... \quad (9)$$

Here the capacitance C will be $C = \epsilon_0\epsilon_r/d$. ϵ is the dielectric constant and d is the thikness of layers.

Our capacitance model can be represent by the following figure;

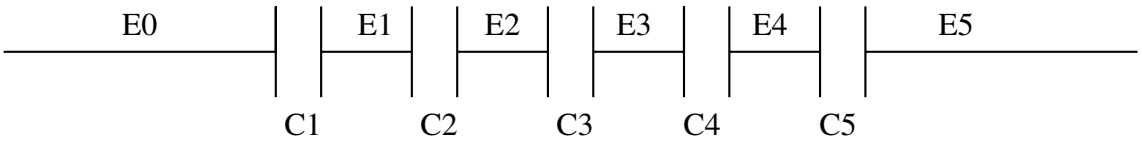

Figure 12: Capacitance Model of Device

Here C_1 is the capacitance in between the left gate SiO_2 layer and Graphene layer, C_2 is the capacitor in between Graphene layer and $h - BN$ layer.C_3 is the capacitor in between $h - BN$ layer and Graphere layer, C_4 is the capacitor in between $h-BN$ layer and Graphere layer.C_5 is the capacitor in between Graphene layer and right SiO_2 layer.

As we get the generalized equation so we can now find out the specific equation of charge at different level of our modeled device. Here we can use $E^{vac} = E$

for simplification and the charge at different layer the specific equation will be as follows;

$$Q_o = C_1E_o - C_1E_o \tag{10}$$

$$Q_1 = -C_1E_o + (C_1 + C_2)E_1 - C_2E_2 \tag{11}$$

$$Q_2 = -C_2E_1 + (C_2 + C_3)E_3 - C_3E_3 \tag{12}$$

$$Q_3 = -C_3E_2 + (C_3 + C_4)E_3 - C_4E_4 \tag{13}$$

$$Q_4 = -C_4E_3 + (C_4 + C_5)E_4 - C_5E_5 \tag{14}$$

$$Q_5 = -C_5E_4 + (C_5 + C_6)E_5 - C_6E_6 \tag{15}$$

So from these equations we can simplified it and the simplification leads us to the following matrix:

$$\begin{bmatrix} C_1 & -C_1 & & & & \\ -C_1 & C_1 + C_2 & -C_2 & & & \\ & -C_2 & C_2 + C_3 & -C_3 & & \\ & & -C_3 & C_3 + C_4 & -C_4 & \\ & & & -C_4 & C_4 + C_5 & C_5 \\ & & & & -C_5 & C_5 \end{bmatrix} \begin{bmatrix} E_o \\ E_1 \\ E_2 \\ E_3 \\ E_4 \\ E_5 \end{bmatrix} = \begin{bmatrix} -eQ_o \\ -eQ_1 \\ -eQ_2 \\ -eQ_3 \\ -eQ_4 \\ -eQ_5 \end{bmatrix}$$

So from this matrix we can form matrix-2 to find E_0 to E_5 by simplifying this matrix.

$$\begin{bmatrix} E_1 \\ E_2 \\ E_3 \\ E_4 \\ E_5 \end{bmatrix} = \begin{bmatrix} C_1 + C_1 & -C_2 & & & \\ -C_2 & C_2 + C_3 & -C_3 & & \\ & -C_3 & C_3 + C_4 & -C_4 & \\ & & -C_4 & C_4 + C_5 & -C_5 \\ & & & -C_5 & C_5 \end{bmatrix}^{-1} \begin{bmatrix} -eQ_1 + C_1 E_0 \\ -eQ_2 \\ -eQ_3 \\ -eQ_4 \\ -eQ_5 \end{bmatrix}$$

Here $E_0 = -eV_g + \phi_g$ and ϕ_g is the bottom gate work function. From the matrix we can get the value of E_i and with that value we can calculate the charge density. To calculate the charge density we use the following equation:

$$Q_i = -e \int_{U_i}^{\infty} D_i(E) f_i^e(E) dE + e \int_{-\infty}^{U_i} D_i(E) f_i^p(E) dE \tag{16}$$

For the above equation

$$U_i = E_i - \phi_i \tag{17}$$

For equation-17

$$E_1 = E_s^{dir} \tag{18}$$

$$E_2 = E_3 = E_4 = E^{mid} \tag{19}$$

$$E_5 = E_D^{dir} \tag{20}$$

where E_s^{dir} is the source Dirac-point energy, E^{mid} is the channel midgap energy and E_D^{dir} is the drain Direc-point energy.

Again for the equation-8 D is the density of states and $f^{e(p)}$ is the electron hole occupancy. Now from matrix 2 and equation-16 are then solved self consistently until U_i converges.

When we applied an arbitrary V_g and V_b is applied according to figure-11 we will get an U_i profile. At finite bias the U_i profile will be as follows:

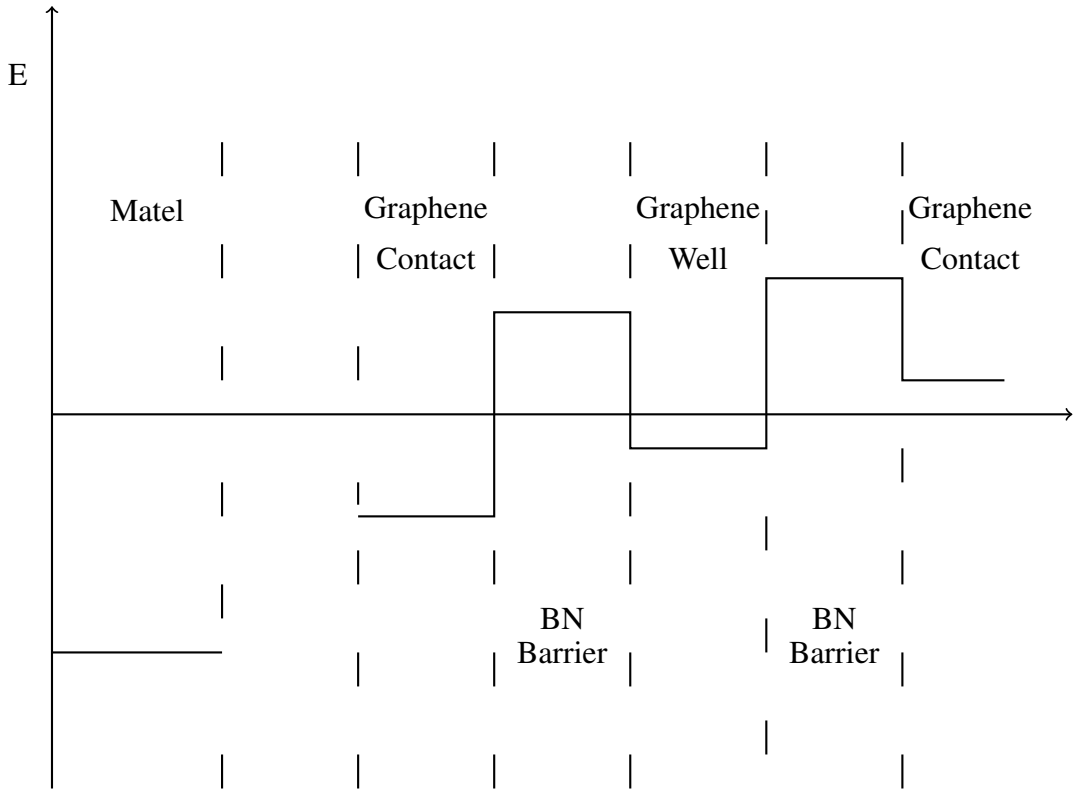

Figure 13: U_i Profile at Finite Bias

In order to finding the U_i profile we use the following parameters for simulation:

SiO_2 insulator thickness, $t_{ins} = 300nm$

SiO_2 dielectric, $\epsilon_{ins} = 4$

The work function of the Si gate, $\phi_g = 4eV$

The work function of the graphene source/drain contacts, $\phi_{SD} = 4.7eV$

The work function of the hBN channel, $\phi_C = 3eV$

The distance between graphene contacts and hBN channel is 0.5nm

hBN and graphene well interlayer distance is 0.35nm

Number of channel layers, $N =$

Here, $U_0 = -eV_g$, $U_1 = E_S^{dir}$, $U_{N+5} = E_D^{dir}$ and U_2 to U_{N+4} is E^{mid}

The electron transport behavior across the device is studied by using NEGF formalism [22]. The Hamiltonian of the mono layer hBN using π-orbital tight binding model is given by

$$H(K) = \begin{bmatrix} E^{mid} + E_{gap}/2 & -t_0 - 2t_0 e^{iK_x} cosK_y \\ -t_0 - 2t_0 e^{-iK_x} cosK_y & E^{mid} - E_{gap}/2 \end{bmatrix}$$

where $K_y = \sqrt{3}k_y a_0/2$, $K_x = 3k_x a_0/2$, itralayer nearest neighbor (NN) hoping parameter, $t_0 = 2.3eV$ [23], bandgap of monolayer hBN, $E_gap = 5eV$ and the NN interlayer atomic distance $a_0 = 0.15$ nm. We use interlayer hoping parameter $t_p = 0.6eV$.

4 Simulation Procedure

To obtain I-V characteristics of the device , quantum transport equation is used using non euilibirum greens function (NEGF) formalism [24] . In order to incorporate the charging effects and to obtain built-in electric field, self-consistent capacitor model and the transport equation are self-consistently solved. the carrier dymanics is explained as retarded Greens function , G^R, Under NEGF formalism. The function under steady state condition can be shown as

$$G^R(E) = \left[(E + i\eta)I - H_0 - \sum_S^R - \sum_D^R\right]^{-1} \tag{21}$$

H_0= Device Hamiltonion

$\sum_{S(D)}^R$=self-energy term due to the sourse (drain) contact.

The effect of electron-phonon and electron-electron interactions can be included by combining the extra self-energy terms [20] in equation-21, which are omitted for simplicity. I is the matrix, and η is a small number who helps to activate the energy-level broadening effects.

The electron and hole statistics are explained by correlation function shown in below:

$$G^n(E) = G^R(E)\left[\sum_S^{in} + \sum_D^{in}\right] G^{R^\dagger}(E) \tag{22}$$

$$G^p(E) = G^R(E)\left[\sum_S^{out} + \sum_D^{out}\right] G^{R^\dagger}(E) \tag{23}$$

The contact in/out-scattering term are calculated from the energy-level broadening function, $\Gamma_{S(D)} = i\left[\sum_{S(D)}^R - \sum_{S(D)}^{R^\dagger}\right]$, due to source (drain) contact using some equations written in follows:

$$\sum_S^{in} = f_S\Gamma_S, \sum_D^{in} = f_D\Gamma_D, \sum_S^{out} = (1 - f_S)\Gamma_S$$
$$\sum_D^{out} = (1 - f_D)\Gamma_D$$

Where f_S and f_D are the source and drain Fermi function, respectively. Density of states (DOS) at the j^{th} atomic site can be defined as

$$\rho_j(E) = \frac{1}{2\pi} A_{j,j}(E) \tag{24}$$

Where $A = i(G^R - G^{R^\dagger})$ is called spectral function. Then, electron (hole) density at the j^{th} atomic site can be calculated as follows:

$$n_j^{e(p)} = \frac{1}{\pi} \int_{U_i(-\infty)}^{\infty(U_i)} G_{j,j}^{n(p)}(E) dE \tag{25}$$

where E_{nj} is the charge charge neutrality . point [21] at the jth atomic site and calculated by exploring two integers over DOS at each atomic site using a trail energy value, E_{nj} as upper bound for valence states and lower bound for conduction sates in search of equal distribution, the electrostatic potential distribution is determined using Poisson as follows:

$$\nabla^2 U_j = \frac{q(n_j^e - n_j^h)}{\epsilon a \Delta z} \tag{26}$$

where U_j is the Hartree potential at the jth atomic site, ϵ is the permittivity of channel material, a is the effective are per atomic site and z-axis grid spacing $\Delta z = 0.5a_{c-c}$. The equation is solved under 3-D discretization using the finite-difference method. For source, drain and gate contacts, boundary condition is Drichlet (as the potential is fixed in contacts). In addition, in open faces of GNR sheet and oxide, the boundary condition is Neumann which is an open boundary.

5 Result

5.1 Finding the Value of Capacitances

After completing our simulation we found the capacitances value as follows:

$$C_1 = 1.1805e^{-04} \text{ nF}$$

$$C_2 = 0.0177 \text{ nF}$$

$$C_3 = 0.0253 \text{ nF}$$

$$C_4 = 0.0253 \text{ nF}$$

$$C_5 = 0.0177 \text{ nF}$$

Where,

C_1 is the capacitance between SiO_2 and Graphene contact layer

C_2 is the capacitance between Graphene contact layer and hBn barrier layer

C_3 is the capacitance between hBN barrier and Graphene well layer

C_4 is the capacitance between Graphene well layer and hBN barrier layer

C_5 is the capacitance between hBN barrier and Graphene contact layer

5.2 V_D vs I_D Curve Observation

We did the simulation for $V_G = V_{FB} + X$ where X is the various voltage we applied at the gate side of our device.

Now for $X = 0V$ we get the I_D vs V_D curve as follows:

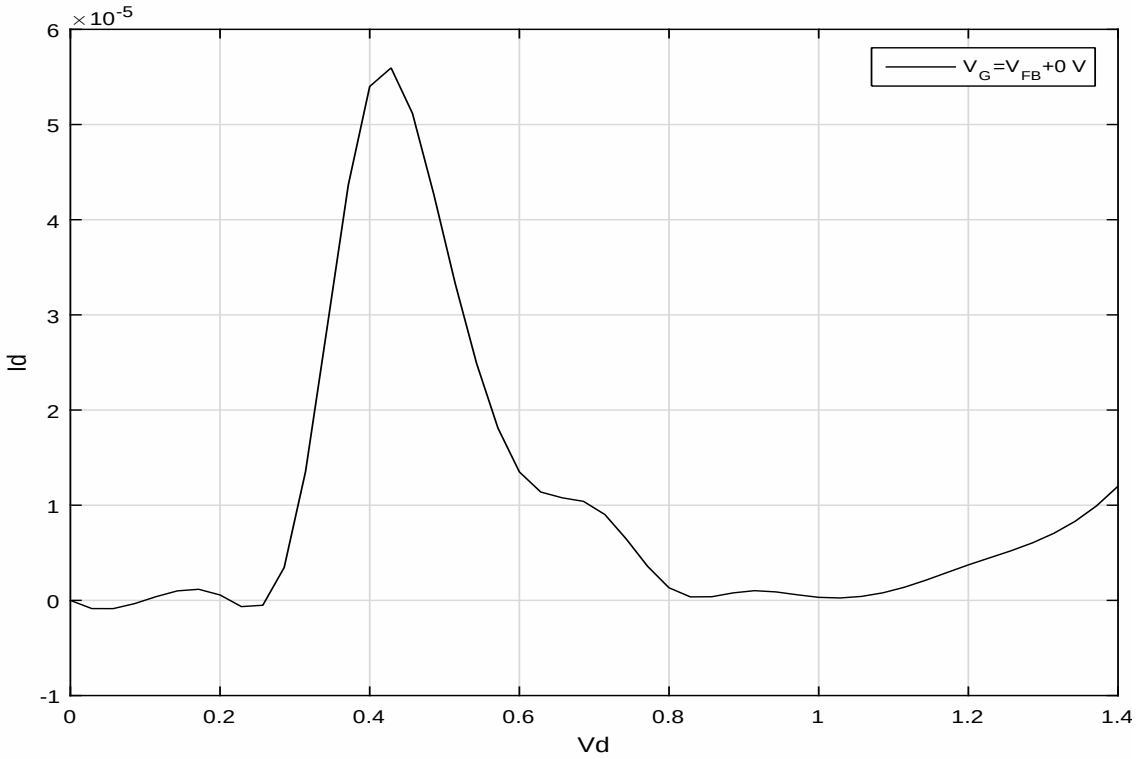

Figure 14: I_D vs V_D Characteristics of Our Device at $V_G = V_{FB} + 0V$

After this we increase the value of X to $0.5V$ then the I_D vs V_D curve came as follows:

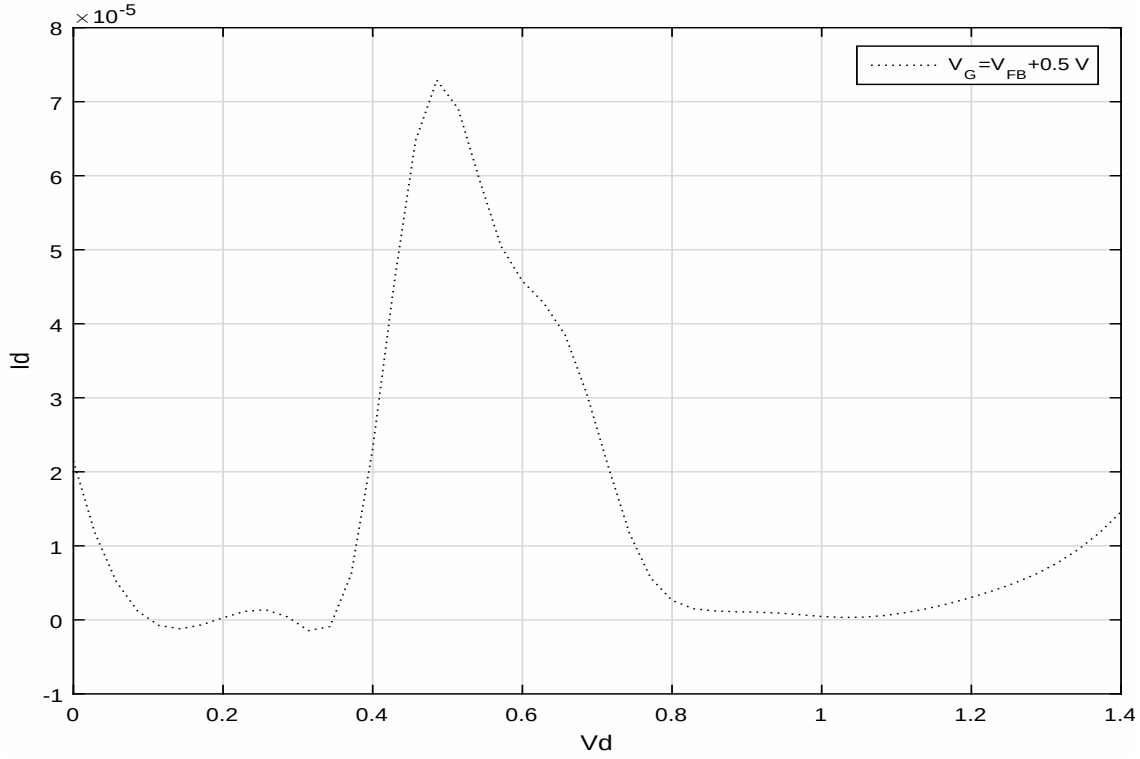

Figure 15: I_D vs V_D Characteristics of Our Device at $V_G = V_{FB} + 0.5V$

After this we further increase the value of X to $0.75V$ then the I_D vs V_D curve came as follows:

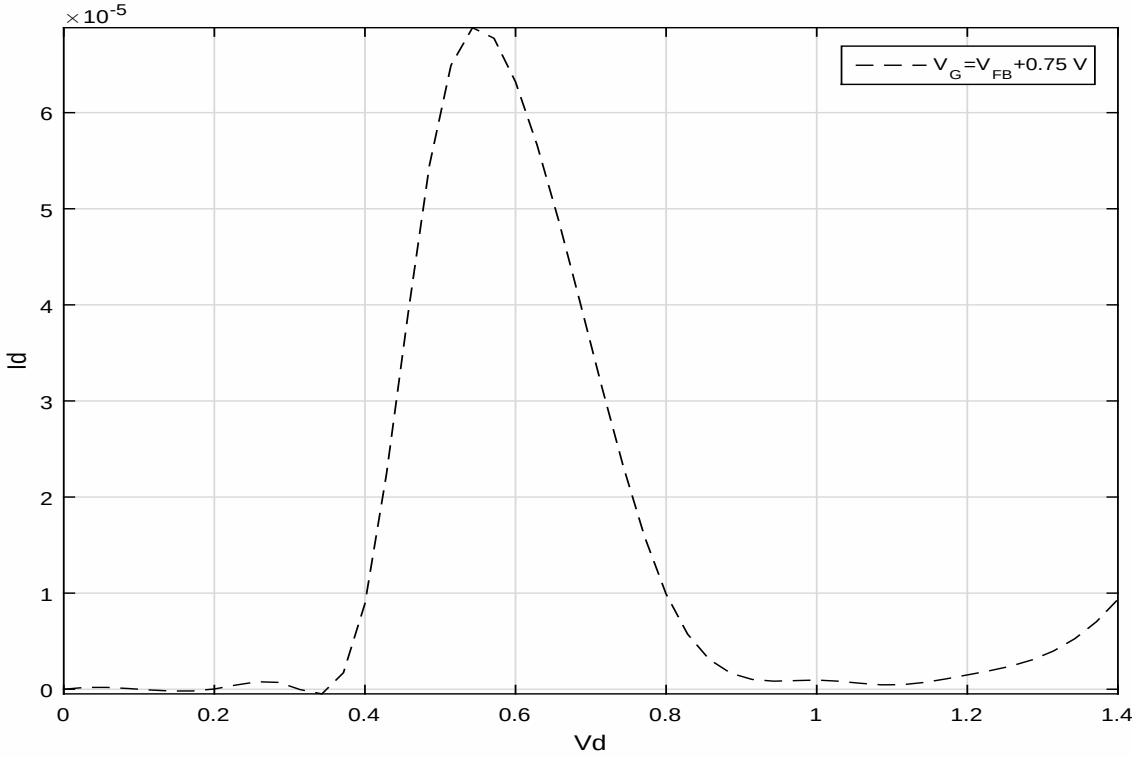

Figure 16: I_D vs V_D Characteristics of Our Device at $V_G = V_{FB} + 0.75V$

If we emerge the three IV characteristics then we find the graph as follows;

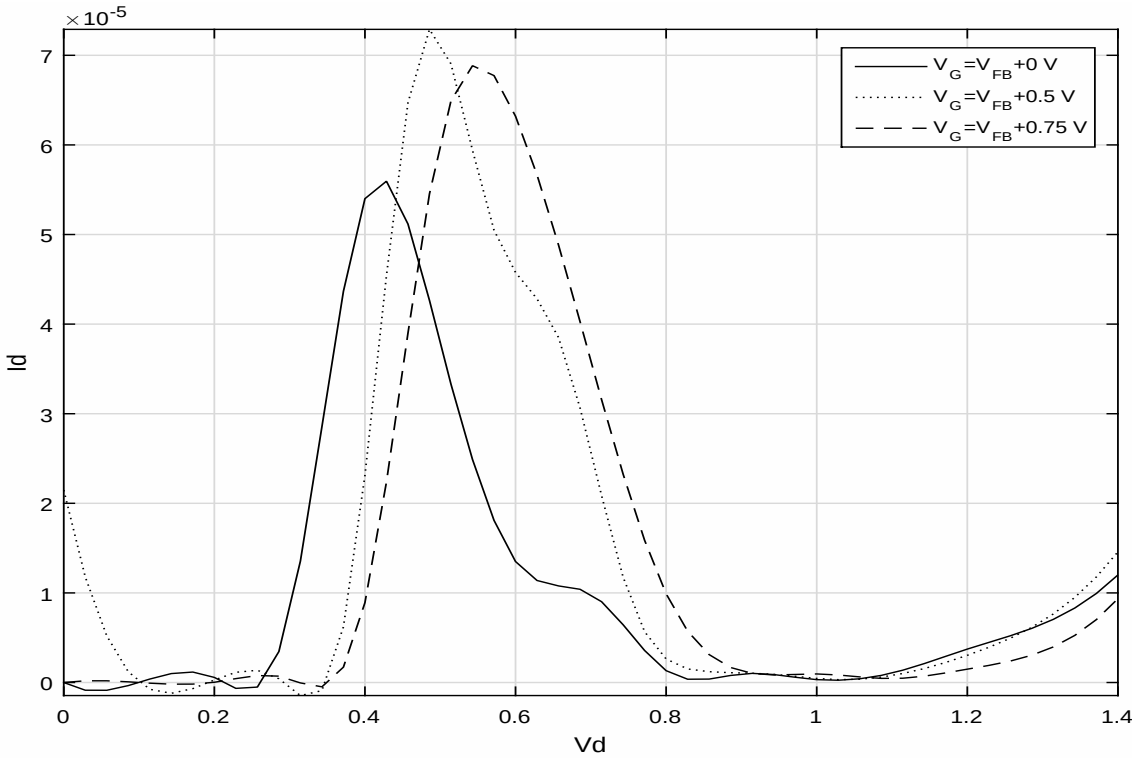

Figure 17: I_D vs V_D Characteristics of Our Device

From here we can see that the current at different gate voltage shows different characteristics. From this we can found that our modeled device shows the characteristics of RTD as it shows peak and valley in its characteristics. We also can determine when it will give us increasing current characteristics and when it will give a decreasing current characteristics. At different V_D it shows different characteristics.

5.3 Electron Tunneling Transportation Due to Different Voltage V_D

Now from the I_D and V_D if we make different segment of the whole figure-17 into three zone like zone-1 for $0V \leq V_D \leq 0.4V$, zone-2 for $0.4V \leq V_D \leq 0.8V$ and zone-3 for $V_D \geq 1.2V$ then we can explain the electron tunneling transportation by using Fig-13. After making the segment of the figure-17 the figure is become as follows:

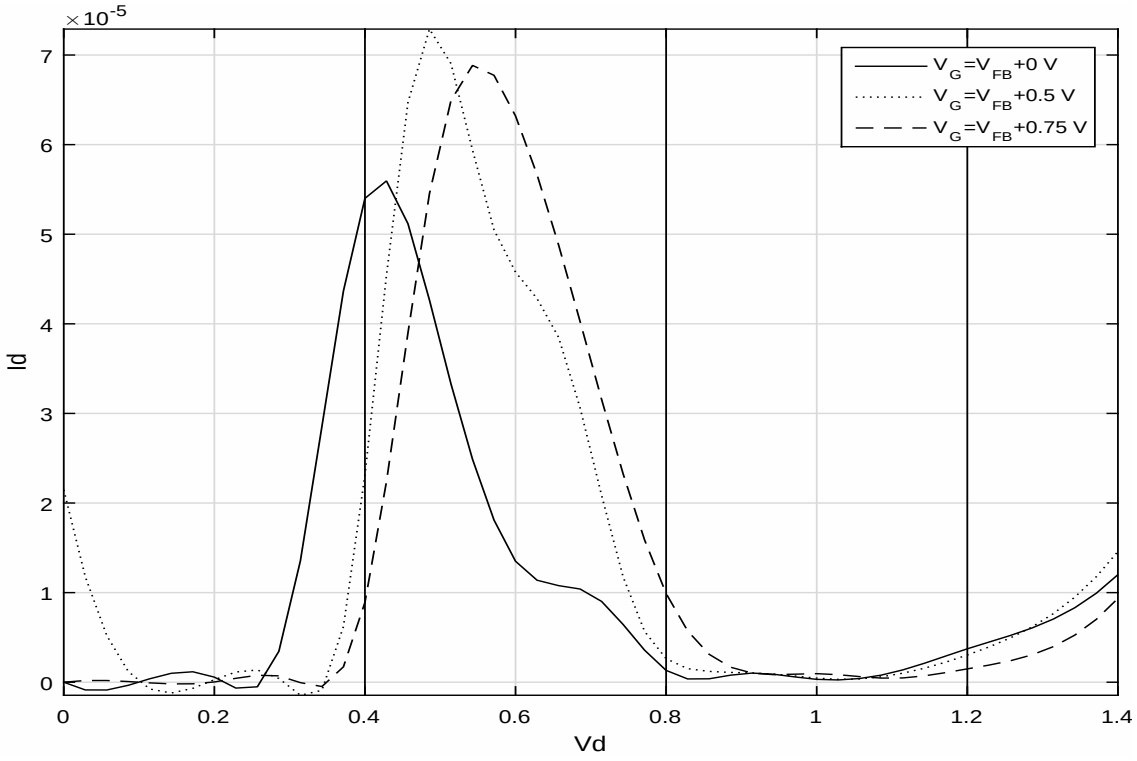

Figure 18: I_D vs V_D Plot After segmentation

After applying different value of V_D we observe the resonant tunneling electron transportation scenario in our modeled device. We found some scenario as

follows:

5.3.1 At $V_D = 0V$

For electron flow electrons need much energy so that they could overcome the energy of the barrier but here as we are giving $V_D = 0V$ electrons are not getting much energy to cross the barrier so here no current will flow , $I_D = 0A$.

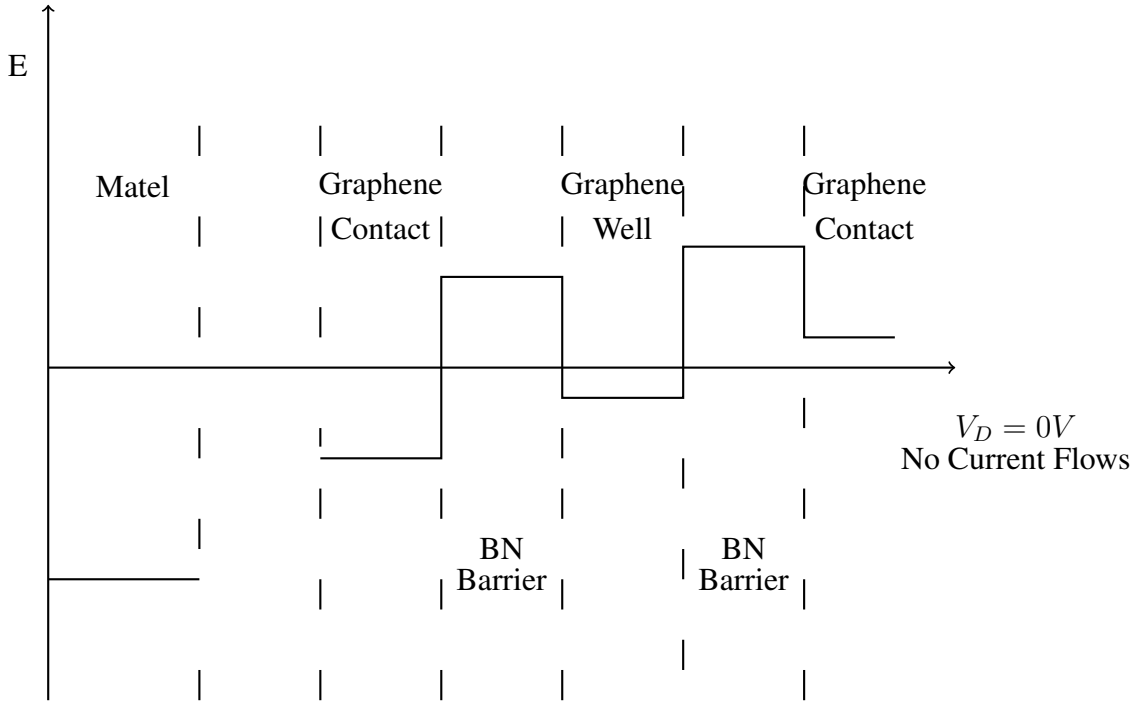

Figure 19: At $V_D = 0V$

5.3.2 At $V_D = (0 \rightarrow 0.4)V$

When we applied drain voltage grater than $V_D = 0V$, due to having very small particle potential of electrons grater than the barrier potential, some electron will tunnel through the two tunneling barriers and current starts to increase with the increasing V_D. And this type of behavior continuous upto $V_D = 0.4V$ For this reason we will get steeper exponentially increased current for $V_D = (0 \rightarrow 0.4)V$. this characteristic is shown in $Fig - 18$

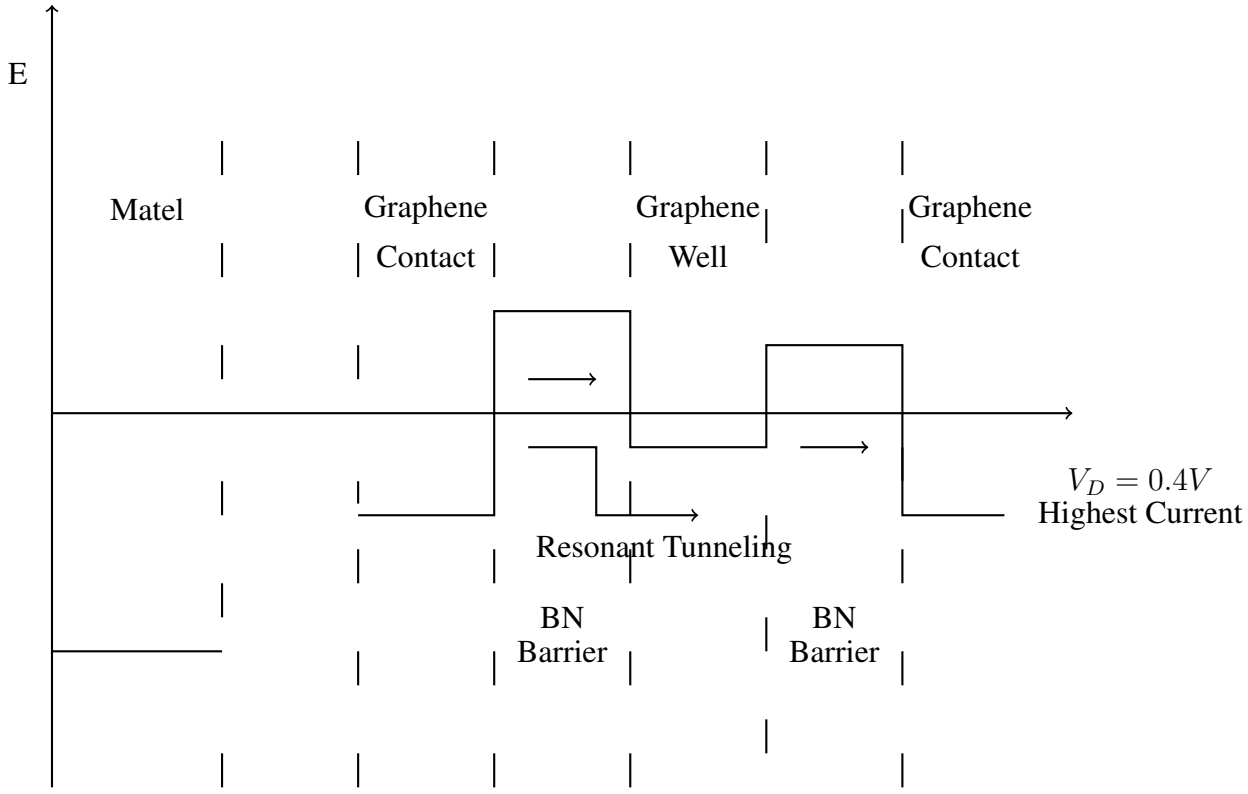

Figure 20: At $V_D = 0.4V$

5.3.3 At $V_D = (0.4 \rightarrow 0.8)V$

We can see from the $Fig - 18$,if we give some potential at the drain side greater than $0.4V$ up to $0.5V$ then the electrons will get more energy and has it's highest current in between $0.4V$ and $0.5V$. When we increase the V_D from $0.5V$ to $0.8V$ the energy of electrons will cross the quasi energy level and thus the current will start to decrease.

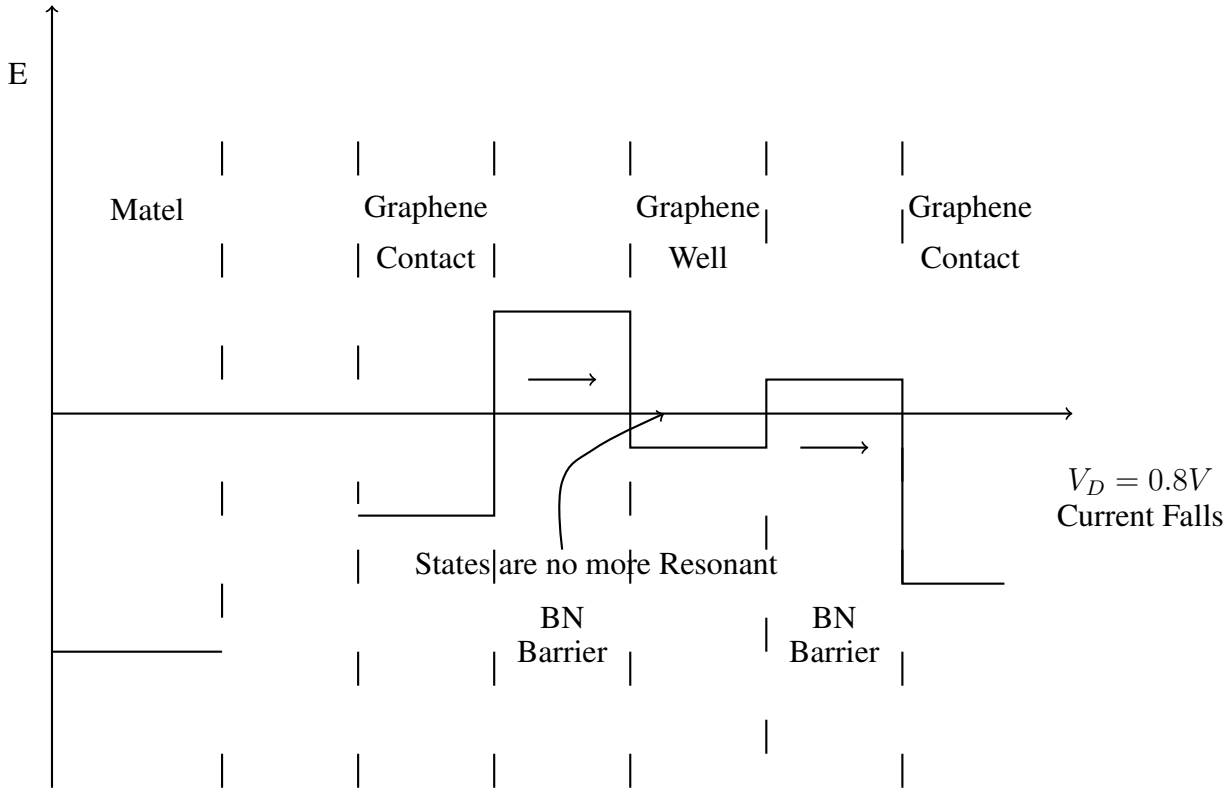

Figure 21: At $V_D = 0.8V$

5.3.4 At $V_D > 1.2V$

If we increase further voltage at the drain side then electrons will get more energy So as we increase the voltage at our device from $V_D = 0.8V$ to $1.2V$ there no significant change in current is not visible. But when we further increase by$V_D = 1.2V$ we can see from the graph that our current starts to increase again.

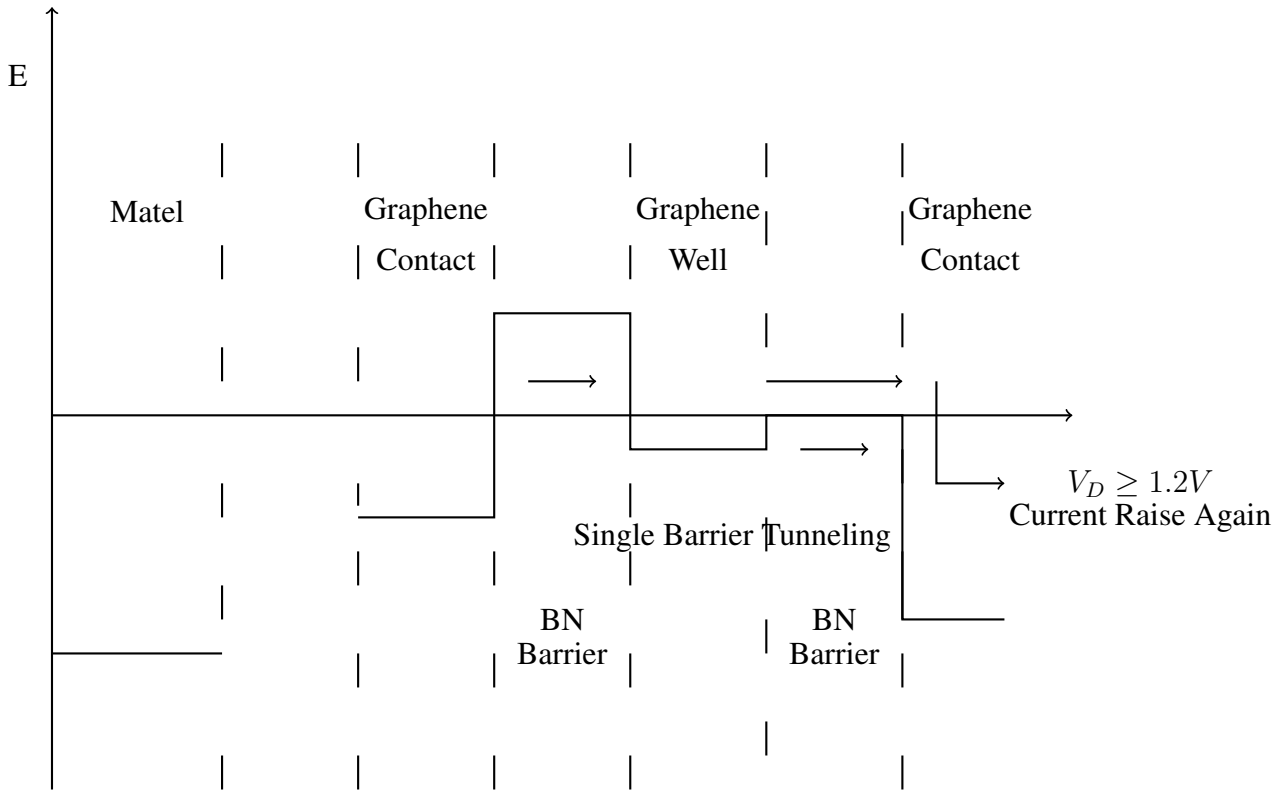

Figure 22: At Further Increased Voltage

5.4 Decision

So from tis result we can say that our device is showing the characteristics of RTD. It will work as heterojunction Van der Wells resonant tunneling diode.

6 Conclution

A resonant tunneling structured diode called Resonant Tunneling Diode (RTD) has been already proven a better option as a replacement of TD or CMOS which id a upgraded version of TD.A feature of RTD is that it gives faster operation than TD. Beside this there is a major advantage in RTD over TD and that is when a high reverse bias voltage is applied to TDs, there is very high leakage current and at the RTD side there we could nd different amount of leakage current depending on the material used for the RTD.Additionally it contains a very solitary property called Negative Differential Resistance (NDR) which is very large at room temperature. we also get different electronic properties from RTD by fabricating RTD in different types of resonant tunneling structure such as heavily doped PN junction in Esaki diodes, double barriers and triple barriers along with various kinds of elements like as type IV,III-V, II-IV semiconductors and it is suited for the design of highly compact, self-latching logic circuits and so more. RTD has proven fruitful in the development of a gate-level pipelining technique,(nanopipelining)by significantly improving speed of pipelined systems. the working principle of RTD depends on biasing voltage V_D, where for different biasing voltage RTd shows variety in it's characteristics like increasing current , peak current ,deceasing current and the again increasing.

In our device, we have used 2 layers of Boron nitride a hexagonal lattice consisting of analogous structure, material as our tunneling barrier and both side of the barriers two Graphene contact are used and a graphene is sandwiched by monolayer BN is predicted to have a tunable bandgap without sacrificing its mobility.

Two band structure calculation methodologies called Density Functional Theory (DFT) and nearest Tight Binding (TB) method have been particularly used in this paper in order to nd appropriate bandgap of the two concerned materials. The name Density Functional Theory (DFT) has been driven from the fact that DFT incorporates the use of functional s of the electron density and DFT also a cost effective method. And nearest Tight Binding method calculates electronic band structures using approximate set of wave functions based on superposition of wave functions for isolated atoms located at each atomic site.

In our work we build RTD by graphene and hBN layers using the self-consistent capacitive model which consists of two tunneling channel made of layered hBN sandwiched between three graphene layers.To estimate the electrochemical potential at graphene and hBN, a self-consistent capacitance model is used.

Finally To obtain I-V characteristics of the device , quantum transport equation is used using non euilibirum greens function (NEGF) formalism. to observe charging effect and built in potential, self-consistent capacitor model and the transport equation are also self-consistently solved. And after completing our overall simulation by applying different voltages, we observe electron tunneling transportation. And the achieved I-V characteristic curve of our Graphene Boron Nitride Vertical Heterojunction Van der Waals Resonant Tunneling Diode shows the similar characteristics of a conventional RTD where the peak and valley current is visible.

7 References

[1] Ling, Johnny. Resonant Tunneling Diodes: Theory of Operation and Applications (n.d.): n. pag. Web. http://www.ece.rochester.edu/courses/ECE423/ECE223$_4$23$_M$SC426

[2]https://www2.warwick.ac.uk/fac/sci/physics/current/postgraduate/regs/mpags/ex5/devices/rtd/

[3] Saumitra Raj Mehrotra; Gerhard Klimeck (2010), "Resonant Tunneling Diode operation," https://nanohub.org/resources/8799.

[4] Maezawa, K. "Resonant Tunneling Diodes and Their Application to High-speed Circuits." IEEE Compound Semiconductor Integrated Circuit Symposium, 2005. CSIC '05. (2005)

[5] Ghosh, R. K., Lin, Y. C., Robinson, J. A., Datta, S. (2015). Heterojunction resonant tunneling diode at the atomic limit. International Conference on Simulation of Semiconductor Processes and Devices (SISPAD).

[6] Kumar, S. B., Seol, G., Guo, J. (2012). Modeling of a vertical tunneling graphene heterojunction field-effect transistor. American Institute of Physics, 101(3)

[7] Uemura, T., Mazumder, P. (1999). Design and Analysis of Resonant Tunneling Diode based High Performance System. IEICE Trans. Electron, E82-C

[8] https://en.wikipedia.org/wiki/Tunnel$_d iode$.

[9] A. Pakdel, D. Golberg, Chem. Soc. Review, 43 (2014) 934-959.

[10] M. K. Denk, Inorganic Chemistry (2000)

[11] H. Hiura, Appl. Surf. Sci. 222 (2004) 374.

[12] C. Berger, Z. Song, T. Li, X. Li, A. Y. Ogbazghi, R. Feng, Z. Dai, A.N. Marchenkov, E.H. Conrad, P.N. First, W.A. de Heer, J. Phys. Chem. B 108

(2004) 19912

[13] Y. Zhang, Y.W. Tan, H.L. Stormer, P. Kim, Nature (London) 438 (2005) 201

[14] K.S. Novoselov, A.K. Geim, S.V. Morozov, D. Jiang, M.I. Katsnelson, I.V. Grigorieva, S.V. Dubonos, A.A. Firsov, Nature (London) 438 (2005) 197

[15] N. Kerszberq and P. Suryanarayana, RSC Adv., 5, (2015) 43810-43814

[16] K. Zhao, M. Zhao, Z. Wang, Y. Fan, Phys. Rev. E 43 (2010) 440-445

[17] M. Topsakal, E. Akturk, S. Ciraci, Phys. Rev. B 79 (2009) 115442.

[18] C.H. Park, S.G. Louie, NanoLett. 8 (2008) 2200.

[19] Z. Zhang, W. Guo, Phys. Rev. B 77 (2008) 075403.

[20] M. Pourfath, The Non-Equilibrium Greens Function Method for Nanoscale Device Simulation. Vienna, Austria: Springer-Verlag, 2014.

[21] A. H. C. Neto, F. Guinea, N. M. R. Peres, K. S. Novoselov, and A. K. Geim, The electronic properties of graphene, Rev. Mod. Phys.,vol. 81, no. 1, p. 109, Jan. 2009.

[22] S. Datta, Quantum Transport: Atom to Transistor (Cambridge University Press, Cambridge, 2005).

[23] R. M. Ribeiro and N. M. R. Peres, Phys. Rev. B 83(23), 235312 (2011).

[24] S. Datta, Nanoscale device modeling: The Greens function method, Superlattices Microstruct., vol. 28, no. 4, pp. 253278, Oct. 2000.